

A viscometric approach of pH effect on hydrodynamic properties of human serum albumin in the normal form

Karol Monkos

Department of Biophysics, Medical University of Silesia, H. Jordana 19, 41-808 Zabrze 8, Poland

Abstract. The paper presents the results of viscosity determinations on aqueous solutions of human serum albumin (HSA) at isoelectric point over a wide range of concentrations and at temperatures ranging from 5°C to 45°C. On the basis of a modified Arrhenius equation and Mooney's formula some hydrodynamic parameters were obtained. They are compared with those previously obtained for HSA in solutions at neutral pH. The activation energy and entropy of viscous flow and the intrinsic viscosity reach a maximum value, and the effective specific volume, the self-crowding factor and the Huggins coefficient a minimum value in solutions at isoelectric point. Using the dimensionless parameter $[\eta]c$, the existence of three ranges of concentrations: diluted, semi-diluted and concentrated, was shown. By applying Lefebvre's relation for the relative viscosity in the semi-dilute regime, the Mark-Houwink-Kuhn-Sakurada (MHKS) exponent was established. The analysis of the results obtained from the three ranges of concentrations showed that both conformation and stiffness of HSA molecules in solutions at isoelectric point and at neutral pH are the same.

Key words: Human serum albumin — Activation energy — Effective specific volume — Intrinsic viscosity — Huggins coefficient — Mark-Houwink-Kuhn-Sakurada exponent

Introduction

Human serum albumin (HSA) is the most abundant human blood plasma protein, but it can also be found in all tissues and body fluids. It contributes to colloidal osmotic blood pressure, but mainly serves as a transport protein for fatty acids, hormones, metal ions, and amino acids, as well as pharmaceutical compounds (Peters 1996). The X-ray crystallographic analysis of HSA revealed that protein is a 585 amino acid residue monomer that folds into three structurally homologous α -helical domains (He and Carter 1992). Each domain is divided into two subdomains which share common structural elements (Gelamo et al. 2002). In the crystal state these three homologous domains assemble to form a heart-shaped molecule. However, in solution the environment of HSA is different than in the crystal state and the protein undergoes reversible conformational transformations with change in pH (Amiri et al. 2010; Otosu et al. 2010;

Chilom et al. 2011). The normal (or N) form is predominant from pH 4.3 to 8.0. First conformational transition is recognized at pH 4.3 when HSA conformation changes to highly charged fast migrating form (or F). At pH less than 2.7 the F-form changes to the fully extended form (or E). On the other side of pH, a conformational transition of HSA takes place at pH 8.0 when the N-form changes to basic form (or B). A conformation of HSA in the normal form is commonly approximated by an ellipsoid of revolution with one long semi-axis (a) and two shorter semi-axes (b). It appears that quite different models and values of "a" and "b" are taken by authors to interpret different experimental data (Young 1963; Peters 1985; Menon and Allen 1990; Sjöberg and Mortensen 1994; Ladam et al. 2000). However, analysis of those models showed that from a hydrodynamic point of view the hydrated HSA molecules in the N-form can be treated as a prolate ellipsoid of revolution with the effective semi-axes $a_h = 8.2$ nm and $b_h = 2.1$ nm (Monkos 2004).

HSA is probably one of the most studied models of globular proteins and is the subject of many physicochemical studies. In recent years the studies mainly focus on the investigations of mechanisms of binding of HSA with different molecules and atoms, but are also directed at the

Correspondence to: Karol Monkos, Department of Biophysics, Medical University of Silesia, H. Jordana 19, 41-808 Zabrze 8, Poland
E-mail: monkos@sum.edu.pl

determinations of the hydration, thermal stability, denaturation, interactions and other functional properties of HSA. The studies explore many different experimental techniques such as X-ray diffraction (He and Carter 1992; Olivieri and Craievich 1995; Bhattacharya et al. 2000), infrared spectroscopy (Bramanti and Benedetti 1994), ¹H-NMR spectroscopy (Menon and Allen 1990; Baranowska and Olszewski 1996; Pouliquen and Gallois 2001), EPR spectroscopy (Junk et al. 2011), phase-fluorometry (Buzády et al. 2001), small-angle neutron scattering (Sjöberg and Mortensen 1994), electrospray mass spectrometry (Amoresano et al. 1998), photon correlation spectroscopy (Sontum and Christiansen 1997), differential scanning calorimetry (Picó 1997), circular dichroism spectroscopy (Matei et al. 2011), fluorescence (Vos et al. 1987; Gelamo et al. 2002; Kamal and Behere 2002) and viscometry (Monkos 2004). There are very few papers dealing with the influence of the pH of a solution on the physicochemical properties of HSA. They are mainly devoted to the problems of influence of different values of pH on mechanisms of binding of HSA with different markers (Vlasova and Saletsky 2009; Vlasova et al. 2010, 2011). However, as far as I know, there is no paper in which the influence of the pH on the hydrodynamic properties of HSA would be explored.

This work presents the results of viscosity measurements for aqueous solutions of HSA at isoelectric point (pH 4.7), at temperatures ranging from 5°C to 45°C and over a wide range of concentrations. The viscosity-temperature dependence, for a fixed concentration, is analyzed on the basis of the three parameters modified Arrhenius equation. From this equation, an activation energy and entropy of viscous flow, and the effective specific volume of the HSA are established. At low concentrations, the intrinsic viscosity and the Huggins coefficient are determined. Using the dimensionless parameter $[\eta]c$, where $[\eta]$ is the intrinsic viscosity and c denotes the solute concentration, the existence of three characteristic ranges of concentrations: diluted, semi-diluted and concentrated, on the log-log plot of the specific viscosity *versus* $[\eta]c$ is shown. The obtained results are compared with those obtained earlier for HSA aqueous solutions at neutral pH (7.0) (Monkos 2004), i.e. at pH in the vicinity of physiological pH (7.4) (Vlasova et al. 2011).

Materials and Methods

The HSA (lyophilized, purity 99% and essentially fatty acid- and globulin-free) was purchased from Polish Chemical Reagents factories and was used without further purification for all measurements. From the crystalline state the HSA was dissolved in distilled water. To remove possible undissolved dust particles the solutions were filtered by means of filter papers. The solutions were cooled in a refrigerator up to

4°C until just prior to viscometry measurements, when they were warmed from 5°C to 45°C, mainly by steps of 5°C. The pH values of thus prepared solutions, in the whole range of concentrations, changed slightly with the average value 4.7. This is the isoelectric point for HSA.

Measurements of the viscosity in this study were carried out using an Ubbelohde-type capillary microviscometer. The microviscometer was calibrated using cooled boiled distilled water and a flow time for water was 28.5 s at 25°C. The same microviscometer was used for all measurements and was mounted so that it always occupied the same position in the bath. Water bath was controlled thermostatically at 5–45°C with a precision of $\pm 0.1^\circ\text{C}$. Such a range of temperatures was taken because slightly above 45°C flow times (and viscosities) of HSA solutions increase with increasing temperature. This shows that thermal denaturation of HSA occurs. The temperature of denaturation changes with concentration and, as appeared, the lower the albumin concentration the higher the denaturation temperature. The measurements were mainly conducted in 5°C intervals. Flow times were recorded to within 0.1 s. Solutions of HSA were temperature-equilibrated and passed once through the microviscometer before any measurements were made.

The viscosities of the HSA solutions were measured over a wide range of concentrations, from 9.5 kg/m³ up to 328 kg/m³. Solution densities were measured by weighing. For this purpose, 0.3 ± 0.001 ml of a solution was weighed with the precision of ± 0.1 mg. Albumin concentrations were determined by a dry weight method as described earlier (Monkos and Turczynski 1991).

Results and Discussion

HSA in solutions may exist in the native form only at a narrow range of temperatures. A freezing point of a solution and the denaturation temperature of HSA are the boundaries from the side of low and high temperatures, respectively. At this range, the viscosity-temperature dependence may be quantitatively described by both the Vogel-Tamman-Fulcher's equation (Vinogradov and Malkin 1980), Avramov's relation (Avramov 1998) and the modified Arrhenius formula (Monkos 1996). Because they result from the models which consider the flow mechanism differently, they give different sorts of information about a studied system. In the present work, the discussion of the viscosity-temperature relationship of HSA solutions is limited only to the modified Arrhenius formula. It was successfully applied both for globular (Monkos 1996, 1997, 2000, 2004) and non-globular proteins (Monkos and Turczynski 1999) and has the form:

$$\eta = \exp \left[-\frac{\Delta S_s}{R} + D_s T + \frac{\Delta E_s}{RT} \right] \quad (1)$$

in which η is a solution viscosity; ΔS_s , D_s and ΔE_s are parameters characterizing the solution, R is the gas constant and T denotes absolute temperature. The quantities ΔS_s and ΔE_s are interpreted as the entropy and the activation energy of the process of viscous flow, respectively. The quantity D_s , in turn, describes the rate at which the activation energy decreases with increasing temperature (Monkos 2011). Fig. 1 shows the temperature dependence of the viscosity of HSA aqueous solutions, for some chosen concentrations, at pH 4.7, i.e. at the isoelectric point (pI). To fit the function from Eq. (1) to the experimental values of viscosity, the numerical values of ΔS_s , D_s and ΔE_s are necessary. For each concentration, they were calculated by using the least squares method (Monkos 1996). As seen in Fig. 1 such obtained curves give a good fit to the experimental points over the whole range of temperatures. At zero concentration, Eq. (1) gives the viscosity-temperature dependence for water with the parameters: $\Delta S_s = \Delta S_w = 242 \text{ J/mol}\cdot\text{K}$, $D_s = D_w = 2.55 \times 10^{-2} \text{ K}^{-1}$ and $\Delta E_s = \Delta E_w = 35.8 \text{ kJ/mol}$.

Calculations of the activation energy of a solution for the studied albumin showed that, as for previously studied proteins, ΔE_s monotonically increases with increasing concentration (Fig. 2). This fact can be justified by assuming that the activation energy of a solution is a superposition of the activation energy of water ΔE_w and albumin ΔE_p molecules. As has been shown earlier (Monkos 1996), this leads to the following equation:

$$\Delta E_s = \frac{c}{\alpha - \beta c} (\Delta E_p - \Delta E_w) + \Delta E_w \quad (2)$$

in which $\alpha = \rho_w M_h / M_w$ and $\beta = \alpha \xi - 1$. The quantities ρ_w , ξ , M_h and M_w denote water density in kg/m^3 , the effective specific volume of a protein and the molecular masses of the dissolved proteins and water, respectively. The effective specific volume is the constant of proportionality between the effective molar volume and the molar mass of a macrosolute (Zimmerman and Minton 1993). To calculate the parameters ΔE_p and ξ from the above equation, the molecular mass of hydrated HSA is necessary.

In physiological conditions, proteins exist in water environment and the protein-water interactions influence their structure, function and dynamics. Some water molecules fill the cavities inside proteins and they play an important role in the process of folding of the protein polypeptide chain and in maintaining its stability. Moreover, there exist water molecules ordered on the proteins surface forming a shell of water molecules and having quite different physical properties than those of bulk water molecules (Svergun et al. 1998; Pouliquen and Gallois 2001). These two sorts of water molecules, called “bound” water, migrate with the proteins and contribute to their hydrodynamic mass and volume. In particular, the hydrodynamic mass of protein is the sum of the molecular mass of unhydrated protein M_p and the mass

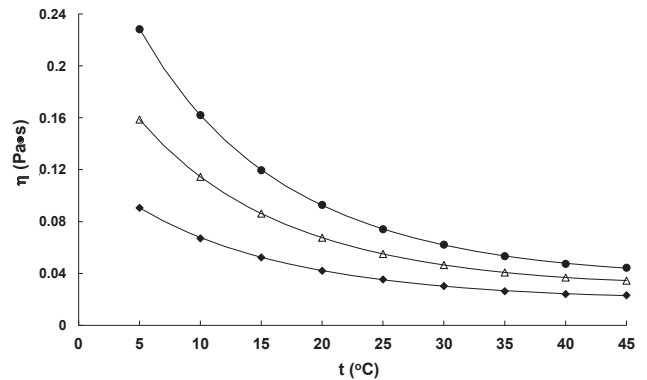


Figure 1. Temperature dependence of the viscosity of HSA aqueous solutions at pH 4.7 for concentrations: $c = 328 \text{ kg/m}^3$ (●), $c = 318 \text{ kg/m}^3$ (Δ) and $c = 293 \text{ kg/m}^3$ (◆). The curves show the fit obtained by using Eq. (1) with the parameters: $\Delta S_s = 1034 \text{ J/mol}\cdot\text{K}$, $D_s = 1.84 \times 10^{-2} \text{ K}^{-1}$ and $\Delta E_s = 165 \text{ kJ/mol}$ for $c = 328 \text{ kg/m}^3$; $\Delta S_s = 1018 \text{ J/mol}\cdot\text{K}$, $D_s = 1.82 \times 10^{-2} \text{ K}^{-1}$ and $\Delta E_s = 162 \text{ kJ/mol}$ for $c = 318 \text{ kg/m}^3$; $\Delta S_s = 905 \text{ J/mol}\cdot\text{K}$, $D_s = 1.6 \times 10^{-2} \text{ K}^{-1}$ and $\Delta E_s = 143 \text{ kJ/mol}$ for $c = 293 \text{ kg/m}^3$.

of “bound” water: $M_h = M_p(1 + \delta)$. The quantity δ means the amount of grams of water associated with the protein *per* gram of protein. It does not depend on temperature (Ferrer et al. 2001) and concentration of a solution (Menon and Allen 1990). For HSA the molecular mass $M_p = 66.479 \text{ kDa}$ (Dockal et al. 1999) and $\delta = 0.379$ (Baranowska and Olszewski 1996). It gives the hydrodynamic mass of HSA $M_h = 91.675 \text{ kDa}$ and $\alpha = 5.093 \times 10^6 \text{ kg/m}^3$.

In Eq. (2) the activation energy and the effective specific volume of HSA must be taken into account as two adjustable parameters. The parameters were calculated by using the least squares method and the following values were obtained: $\Delta E_p = 8.77 \times 10^5 \text{ kJ/mol}$ and $\xi = 1.83 \times 10^{-3} \text{ m}^3/\text{kg}$. As seen in Fig. 2, the function from Eq. (2) gives then a good approximation to the experimental values. In Fig. 2 the activation energy established previously (Monkos 2004) for HSA solutions at neutral pH is also presented. For each fixed concentration, ΔE_s at pI is substantially greater than for a solution at neutral pH. This is because the activation energy of HSA molecules in solutions at pI is substantially greater than in solutions at neutral pH. The activation energy of HSA molecules established in the last case is equal to $\Delta E_p = 1.86 \times 10^5 \text{ kJ/mol}$ (Monkos 2004). It is well-known that the activation energy of dissolved protein depends on its molecular mass (Monkos 2005b; Vinogradov and Malkin 1980). However, it would be interesting to compare the activation energy of different mammalian albumins, which have the similar (or equal) molecular mass. Study of such albumins in solutions outside their pI gave the following values of ΔE_p : $1.27 \times 10^5 \text{ kJ/mol}$ for equine serum albumin, $2.44 \times 10^5 \text{ kJ/mol}$ for porcine serum albumin, $2.66 \times 10^5 \text{ kJ/mol}$ for rabbit serum albumin (Monkos 2005a)

and 2.13×10^5 kJ/mol for ovine serum albumin (Monkos 2005b). Study of bovine serum albumin (BSA) in solutions at pI, in turn, gave the activation energy $\Delta E_p = 5.96 \times 10^5$ kJ/mol (Monkos 1996, 2005b). It appears that there are only small differences between the values of activation energy for albumins in solutions outside the pI. As has been shown in our recent paper (Monkos 2011) in this case the activation energy mainly depends on hydrodynamic radius of albumin. The values of the activation energy of albumins in solutions at pI are substantially greater than those obtained in solutions outside the pI. It strongly suggests that for a given protein the activation energy reaches a maximum value in solutions at pI.

To jump from one equilibrium position to the next, each molecule in liquid has to overcome some potential energy barrier created by neighbouring molecules. The height of this potential energy depends on the strength of intermolecular interactions and establishes the value of the activation energy. Amino acids in proteins are held together by strong covalent bonds along its backbone and by weaker, non-covalent cross-connections. As a result of that the spatial charge distribution of the proteins is usually asymmetric. This asymmetry can be characterized by the dipole moment and higher moments like the lesser investigated quadrupole moment of protein (Laberge 1998). Complexity of the electrostatic properties of proteins causes that the protein-protein interactions are also very complex. At the first approximation, the mean force between proteins created by electrostatic interactions can be expressed as sum of mean forces caused by: the charge-charge interaction, charge-dipole interaction, charge-induced dipole interaction, dipole-dipole interaction, dipole-induced dipole interaction and dispersion interaction (Vilker et al. 1981). Only the first interaction represents repulsive forces. At values of pH, higher than pI of HSA, molecules of HSA are negatively charged as a whole (Vlasova et al. 2010). The Coulomb repulsion between two molecules of HSA partially

balances the attractive forces caused by the remaining interactions. At pH values in the vicinity of (or at) the pI, the net charges on the proteins are small (or equal to zero) and the attractive forces connected with the dipole moment of proteins prevail. Globular proteins have the unusually large dipole moments, in comparison with the dipole moment of water molecules (1.84 D) (Antosiewicz 1995). For example, the dipole moment of HSA and BSA is equal to 700 D and 384 D, respectively (Moser et al. 1966). The values of the activation energy of HSA ($\Delta E_p = 8.77 \times 10^5$ kJ/mol) and BSA ($\Delta E_p = 5.96 \times 10^5$ kJ/mol) obtained in solutions at pI show that the higher value of the dipole moment the higher value of the activation energy of albumin. However, to obtain analytical relation between those quantities more experimental data is needed.

The coefficients ΔS_s and D_s in modified Arrhenius equation depend on concentration in the same manner as ΔE_s , i.e. they monotonically increase with increasing concentration. The experimental values of those parameters for HSA in solutions at pI are presented in Fig. 3. The functional dependence of the parameters on concentration describe the following equations (Monkos 1996):

$$\Delta S_s = \frac{c}{\alpha - \beta c} (\Delta S_p - \Delta S_w) + \Delta S_w \quad (3)$$

$$D_s = \frac{c}{\alpha - \beta c} (D_p - D_w) + D_w \quad (4)$$

in which the pairs of parameters $(\Delta S_p, \xi)$ and (D_p, ξ) are treated as adjustable parameters. By using the least squares method in the above equations, the following values of those parameters were obtained: $\Delta S_p = 5.58 \times 10^6$ J/mol·K, $\xi = 1.78 \times 10^{-3}$ m³/kg and $D_p = 1170$ K⁻¹, $\xi = 1.72 \times 10^{-3}$ m³/kg. As seen in Fig. 3 the functions from Eqs. (3) and (4), with thus obtained values of parameters, give good approximation to the experimental

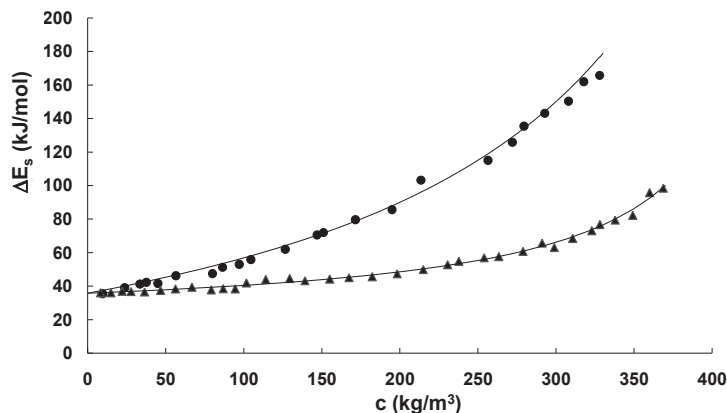


Figure 2. Plot of the solution activation energy ΔE_s vs. concentration c for HSA aqueous solutions at pH 4.7 (●) and pH 7.0 (▲). Experimental points were obtained by using the least squares method. The curves show the fit according to Eq. (2) with $\Delta E_w = 35.8$ kJ/mol and parameters: $\Delta E_p = 8.77 \times 10^5$ kJ/mol, $\xi = 1.83 \times 10^{-3}$ m³/kg for HSA at pH 4.7 and $\Delta E_p = 1.85 \times 10^5$ kJ/mol, $\xi = 2.14 \times 10^{-3}$ m³/kg for HSA at pH 7.0.

values. The values of parameters ΔS_p and D_p established previously for HSA in solutions at neutral pH are 9.57×10^5 J/mol K and 215 K^{-1} , respectively (Monkos 2004). The above results show that for a given protein the parameters ΔS_p and D_p also reach a maximum value in solutions at pI.

Biological systems such as cells and tissues contain a high concentration of macromolecules of one species (as hemoglobin within red cells) or different species (as in cytoplasm). Some types of macromolecules can not individually be present at high concentration, but taken collectively may occupy a substantial fraction of the total volume of the medium (Zimmerman and Minton 1993). Such systems are often called as crowded. Biochemical reactions are usually studied in dilute solutions. However, one can expect that in the crowded environment within cells substantial changes of the parameters characterizing these reactions appear (Zimmerman and Trach 1991). The parameters obtained in conditions of dilute solutions should be replaced for highly concentrated environment of living cells by appropriate activity coefficients. They are a measure of non-ideal behavior arising from interactions between solute molecules. The activity coefficients may be calculated on the basis of the scaled particle theory (Reiss 1965). The results of such calculations for macromolecules modeled as hard spheres are given in the literature (Zimmerman and Trach 1991). It appears that for calculating the activity coefficients the effective specific volume of macromolecules is necessary. There are very few methods which enable to estimate the effective specific volume (Zimmerman and Trach 1991; Zimmerman and Minton 1993). Moreover, they are correct only for macromolecules modeled as hard spheres. The method presented here gives experimental values of the effective specific volume, and without limitations on the macromolecular shape.

The effective specific volume is one of two parameters in Eqs. (2–4). The three values of ξ presented above for

HSA in solutions at pI, differ each other only slightly and give the average value $\langle \xi \rangle = 1.78 \times 10^{-3} \text{ m}^3/\text{kg}$. The effective specific volume for BSA in solutions at pI is very similar: $\xi = 1.62 \times 10^{-3} \text{ m}^3/\text{kg}$ (Monkos 2005a). Contrary to those, experimental values of ξ obtained for albumins in solutions outside the pI are greater: $2.15 \times 10^{-3} \text{ m}^3/\text{kg}$ for HSA (Monkos 2004), $2.32 \times 10^{-3} \text{ m}^3/\text{kg}$ for equine serum albumin, $1.98 \times 10^{-3} \text{ m}^3/\text{kg}$ for rabbit serum albumin, $3.84 \times 10^{-3} \text{ m}^3/\text{kg}$ for porcine serum albumin (Monkos 2005a) and $2.08 \times 10^{-3} \text{ m}^3/\text{kg}$ for ovine serum albumin (Monkos 2005b). These results strongly suggest that the effective specific volume of a protein tends to a minimum value at its pI. This conclusion was partially confirmed by theoretical study (Zimmerman and Minton 1993). In the study albumin molecules are modeled by hard spheres. The results obtained on the basis of analysis of virial expansion show that, in this case, the effective specific volume increases with increasing pH from $0.8 \times 10^{-3} \text{ m}^3/\text{kg}$ (at pH 5.1) up to $1.7 \times 10^{-3} \text{ m}^3/\text{kg}$ (at pH 7.6). As seen, experimental values of ξ are greater than those obtained for hard sphere model. Apart from that the numerical values of ξ for different species of albumin are quite different. Application of experimentally obtained values of the effective specific volume should give more precise values of the activation coefficients. Moreover, for each sort of protein the activation coefficient should be calculated individually.

In recent years the hydrodynamic properties of macromolecules in concentrated suspensions are studied by using both theoretical and experimental methods. Theoretical and simulation studies on diffusion, sedimentation and rheology of porous and core-shell particles in concentrated suspensions have been recently presented in several papers (Abade et al. 2010a,b,c,d, 2011, 2012). In those papers dynamic properties of porous particles, modeled as spheres of uniform permeability, have been studied as a function of their perme-

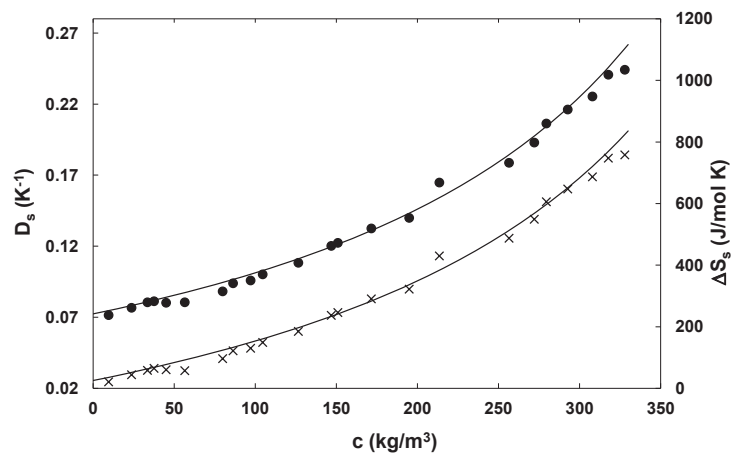


Figure 3. Plot of the parameter D_s (\times) and entropy ΔS_s (\bullet) versus concentration for HSA aqueous solutions at pH 4.7. The points were obtained by using the least squares method; the curves show the fit according to relations (4) and (3), respectively.

ability for the full fluid-phase concentration range. The solvent flow inside the permeable spheres was described by the Debye-Büche-Birnman equation and outside the spheres by the Stokes equation. The calculations of dynamic properties of porous particles in concentrated suspensions are difficult because one has to take into consideration many-particle hydrodynamic interactions mediated by the solvent flow outside and inside the particles. The particles are assumed to interact also non-hydrodynamically by a hard-sphere no-overlap potential. On employing the multipole simulation method encoded in the Hydromultipole program package, the authors calculated with high accuracy sedimentation coefficient (Abade et al. 2010a,b), translational self-diffusion coefficient (Abade et al. 2010a,b, 2011), rotational self-diffusion coefficient (Abade et al. 2011) and high frequency-limiting shear viscosity (Abade et al. 2010c,d) and presented them as functions of concentration and permeability. The most important result of those studies is that the above quantities strongly depend on the permeability. Each of the quantities increases with increasing permeability and this is particularly distinct at higher concentrations. It means that the flow of solvent inside the particles relative to their skeletons leads to a reduction in the hydrodynamic interactions.

The authors used the same method to study dynamic properties of concentrated suspensions of colloidal core-shell particles (Abade et al. 2012). A core-shell particle is composed of a rigid, spherical dry core surrounded by a uniformly solvent-permeable, incompressible shell. The simulations showed that the translational diffusion coefficient decreases with increasing volume fraction, linearly up to volume fraction of about 0.3, and non-linearly for higher values. The decrease of the translational diffusion coefficient with increasing of volume fraction is a consequence of the increasing hydrodynamic interactions between particles. Moreover, the translational diffusion coefficient depends in this case also on a core-to-particle size ratio and on shell permeability. The similar results have been obtained for the rotational diffusion coefficient. The sedimentation coefficient, as translational diffusion coefficient, decreases with increasing volume fraction. However, the most striking difference in the concentration dependence of those quantities is the small sensitivity of the sedimentation coefficient on the shell width, even at high permeabilities. The high-frequency viscosity, in turn, increases with increasing volume fraction and its increase is most pronounced for zero shell width. The results of simulations also showed that the values of the transport coefficients of core-shell particles with a large shell permeability, in concentrated suspensions, depend significantly on the core size.

Small angle X-ray scattering and X-ray photon correlation spectroscopy have been used to study the diffusion properties in concentrated aqueous suspensions of charge-stabilized fluorinated latex spheres at different concentrations and ionic-strength (Gapinski et al. 2007). To the same class of charge-

stabilized suspensions can include proteins and polysaccharides. Diffusion and rheological properties of macromolecules in this case are determined by a interplay of electrostatic and hydrodynamic interparticle forces. The authors showed that all experimental results can be described by using Stokesian dynamics simulation method in combination with a hydrodynamic many-body theory. In particular, the results show that the self-diffusion coefficient of charge-stabilized spheres is larger than its corresponding hard-sphere value. For fixed colloid concentration the self-diffusion coefficient increases with decreasing salt content and the largest value attains in the limit of zero added salt. The most important finding of the paper is that hydrodynamic properties of concentrated charge-stabilized suspensions are explainable by the effect of many-body hydrodynamic interactions. Dynamic light scattering, in turn, has been used to study hydrodynamic properties of suspensions of charged colloidal silica spheres up to the freezing concentration (Holmqvist and Nägele 2010). Like in the previous paper, in interpretation of the experimental data hydrodynamic interactions play an essential role.

Even more complicated situation appears when hydrodynamic properties of macromolecules are studied in the crowded environment. In a recent study (Ando and Skolnick 2010) the authors employed Brownian dynamics simulations to examine possible mechanism responsible for the great reduction in diffusion coefficient of macromolecules *in vivo* from that at infinite dilution. Simulation was performed for a model of an *Escherichia coli* cytoplasm comprised of 15 different macromolecule types at physiological concentrations. Macromolecules were modeled by equivalent sphere representation with an effective radius, i.e. the radius of a sphere with the same volume as the bare protein volume calculated from the specific volume. The results of that simulation show that the large reduction in diffusion coefficient of macromolecules observed *in vivo* can be explained by two factors: excluded volume effects and hydrodynamic interactions. However, nonspecific attractive interactions like van der Waals interactions can also play some role. Average values of short-time and long-time diffusion coefficients obtained by the authors agree only qualitatively with the theoretical values of the self-diffusion coefficients obtained for monodisperse, hard spherical particles (Tukuyama and Oppenheim 1995a,b). The differences in the results obtained by those methods suggest that the heterogeneity of the environment is crucial for understanding crowding effects *in vivo*.

The effect of crowding on the self-diffusion in crowded aqueous solutions of bovine serum albumin was experimentally studied by means of quasielastic backscattering (Roosen-Runge et al. 2011). The same protein was used as tracer molecule and crowding agent. The measurements showed that the translational diffusion coefficient of bovine serum albumin at volume fraction about 0.25 is decreased to 20% of the dilute-limit value. Application of colloid models

to protein diffusion in crowded solutions and interpretation of experimental results led the authors to the conclusion that this reduction is caused solely due to hydrodynamic interactions. These findings are in good accordance with results of simulations discussed above. Moreover, the authors showed that the analysis of colloidal hard-sphere models performed for effective spheres allows on separation of the rotational and translational contribution to the measured diffusion coefficient.

Very recently hydrodynamic properties of BSA in aqueous solutions at physiological concentrations have been the subject of a joint experimental-theoretical study (Heinen et al. 2012). The results obtained from static light scattering, dynamic light scattering, small-angle X-ray scattering and rheometric measurements have been combined with analytical colloid theory. The authors used a simple colloid model in which BSA molecules are approximated by oblate spheroids interacting by a spherically symmetric effective potential. The main quantities discussed in the paper are: low shear-rate static viscosity, static and dynamic scattering function, self-diffusion and collective diffusion coefficients. The letter one describes the cooperative motion of molecules in the direction of thermally induced density gradient. The obtained results prove the influence of salinity on the hydrodynamic properties of BSA. Moreover, the analysis of the results showed that attractive forces between proteins such as the van der Waals forces tend to slow self-diffusion, collective diffusion and sedimentation and to enlarge the viscosity.

In the above discussed papers the authors approximate the macromolecules mainly by hard spheres. In fact many types of macromolecules is more complex. For instance, the shape of proteins is mostly non-spherical and the distribution of hydrophobic surface patches and surface charges is non-isotropic. The irregular protein surface, in turn, causes that protein interaction energy depends on orientation with repulsive and attractive parts. This addi-

tionally complicates the description of hydrodynamically influenced transport properties. To understand processes in the interior of biological cells both experimental results and theoretical studies of biochemical reactions and transport properties of macromolecules in concentrated solutions are highly desirable.

The relative viscosity η_r is defined as the ratio of viscosity of the solution and the solvent. For proteins in aqueous solutions, its dependence on concentration can be quantitatively described by the Mooney equation (Mooney 1951):

$$\eta_r = \exp \left[\frac{S\Phi}{1 - K\Phi} \right] \quad (5)$$

in which Φ denotes the volume fraction of the dissolved proteins, S is the Simha factor and K denotes the self-crowding factor. The volume fraction $\Phi = N_A V_c / M_h$ where N_A and V are Avogadro's number and the hydrodynamic volume of one dissolved protein, respectively. Simha factor depends on the shape of the dissolved proteins and on their hydrodynamic interactions in solution.

The self-crowding factor can be calculated from the relation: $K = (\xi - M_w / \rho_w M_p) \times M_p / N_A V$ (Monkos 1996). It does not depend on temperature. Hydrodynamic volume of one dissolved protein is a sum of a volume of the unhydrated protein and a volume of the hydration shell: $V = V_o + M_p \delta / N_A \rho_w$ (Squire and Himmel 1979). For HSA $V = 155.3 \text{ nm}^3$ (Monkos 2004) and it gives the numerical values of the self-crowding factor: 1.74 in solutions at pH 7 and 2.1 in solutions at neutral pH. In his original paper Mooney showed that values of the self-crowding factor for rigid non-interacting spherical particles should lie in the range (1.35–1.91) (Mooney 1951). However, the results obtained both for globular and non-globular proteins showed that the numerical values of K lie in a broader range (Monkos 1997, 2004, 2005a,b). Moreover, the results presented there and those obtained above for HSA clearly show that – for a given protein – the self-crowding

Table 1. Intrinsic viscosity ($[\eta]$), Mark-Houwink-Kuhn-Sakurada exponent (a), critical concentrations (c^* , c^{**}), reduced critical concentrations ($[\eta]c^*$, $[\eta]c^{**}$) and slopes of the regression lines $\log \eta_{sp}$ versus $\log [\eta]c$ for aqueous solutions of HSA at pH 4.7

T (°C)	$[\eta] \times 10^3$ (m^3/kg)	a	c^* (kg/m^3)	c^{**} (kg/m^3)	$[\eta]c^*$	$[\eta]c^{**}$	Slope $c < c^*$	Slope $c > c^{**}$
5	6.46 ± 0.10	0.333 ± 0.006	32.3 ± 2.4	273 ± 16	0.209 ± 0.020	1.764 ± 0.131	1.109 ± 0.01	8.32 ± 0.26
10	6.30 ± 0.10	0.334 ± 0.007	32.8 ± 2.6	277 ± 11	0.207 ± 0.020	1.741 ± 0.097	1.107 ± 0.01	8.16 ± 0.24
15	6.18 ± 0.10	0.335 ± 0.007	33.1 ± 2.6	277 ± 11	0.204 ± 0.020	1.710 ± 0.094	1.105 ± 0.01	7.93 ± 0.23
20	6.10 ± 0.10	0.336 ± 0.006	33.5 ± 2.6	271 ± 10	0.204 ± 0.019	1.654 ± 0.089	1.104 ± 0.01	7.63 ± 0.25
25	6.06 ± 0.10	0.339 ± 0.006	33.7 ± 2.6	264 ± 10	0.204 ± 0.019	1.602 ± 0.089	1.103 ± 0.01	7.27 ± 0.24
30	6.07 ± 0.11	0.339 ± 0.006	33.8 ± 2.5	268 ± 10	0.205 ± 0.019	1.625 ± 0.090	1.103 ± 0.01	7.12 ± 0.22
35	6.11 ± 0.11	0.345 ± 0.006	33.9 ± 2.5	254 ± 10	0.207 ± 0.019	1.550 ± 0.091	1.102 ± 0.01	6.82 ± 0.27
40	6.18 ± 0.12	0.344 ± 0.006	33.9 ± 2.5	263 ± 10	0.209 ± 0.020	1.627 ± 0.095	1.102 ± 0.01	6.93 ± 0.22
45	6.29 ± 0.13	0.343 ± 0.006	33.5 ± 2.6	281 ± 11	0.211 ± 0.020	1.768 ± 0.104	1.104 ± 0.01	7.24 ± 0.21

Obtained from the fit of the curves in Figs. 4 and 5, and from Eq. (7) and (9). Values are expressed as means \pm SEM.

factor depends on pH and it reaches a minimum value in solutions at pI. It can be partially explained by the fact that K is proportional to the effective specific volume of the protein. Full explanation of the problem should give the theory of viscosity for interacting and aspherical particles.

The Mooney equation – Eq. (5) describes the viscosity-concentration dependence from diluted up to concentrated solutions. In the region of diluted solutions, i.e. in the limit of $c \rightarrow 0$, an expansion of Eq. (5) in the power series of concentration leads to the Huggins relationship:

$$\frac{\eta_{sp}}{c} = [\eta] \{1 + k_1[\eta]c + \dots\} \quad (6)$$

in which $[\eta] = \lim_{c \rightarrow 0} \eta_{sp}/c$ is the intrinsic viscosity, $\eta_{sp} = (\eta_r - 1)$ denotes the specific viscosity and the dimensionless parameter k_1 is the Huggins coefficient. The intrinsic viscosity of a protein measures its contribution to the viscosity of the solution and depends on its hydrodynamic volume occupied in solution. It can be obtained experimentally by using different procedures (Pamies et al. 2008). In the present paper the numerical values of $[\eta]$ have been calculated from the relation (Monkos 1996):

$$[\eta] = \frac{1}{\alpha} \left[-\frac{\Delta S_p - \Delta S_w}{R} + (D_p - D_w) T + \frac{\Delta E_p - \Delta E_w}{RT} \right] \quad (7)$$

and for HSA in solutions at pI they are gathered in Table 1. It is interesting to compare them with the values of $[\eta]$ obtained previously for HSA at neutral pH (Monkos 2004). In this case the intrinsic viscosity decreases from $4.9 \times 10^{-3} \text{ m}^3/\text{kg}$

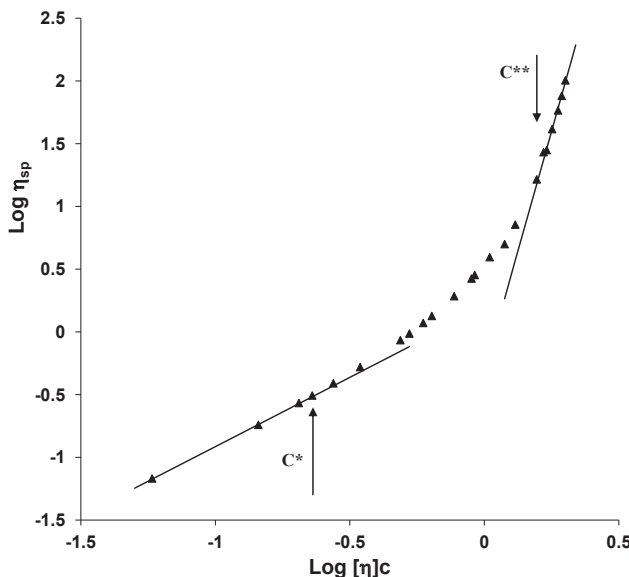


Figure 4. Specific viscosity as a function of $[\eta]c$ in a log-log plot for aqueous solutions of HSA at pH 4.7 and at temperature 20°C; straight lines show different slopes in dilute ($c < c^*$) and concentrated ($c > c^{**}$) regions. The arrows show the boundary concentrations c^* and c^{**} .

($t = 5^\circ\text{C}$) up to $4.61 \times 10^{-3} \text{ m}^3/\text{kg}$ ($t = 45^\circ\text{C}$). It appears that the numerical values of the intrinsic viscosity of HSA at pI are substantially greater than those at neutral pH. However, they are very similar to the values of $[\eta]$ obtained for BSA at pI: $6.49 \times 10^{-3} \text{ m}^3/\text{kg}$ ($t = 5^\circ\text{C}$) and $5.6 \times 10^{-3} \text{ m}^3/\text{kg}$ ($t = 45^\circ\text{C}$) (Monkos 1996). These results suggest that, for a given protein, the intrinsic viscosity reaches maximum value in solutions at pI.

The Huggins coefficient, in turn, can be calculated from the relation (Monkos 1996):

$$k_1 = \frac{1}{2} \left[\frac{2\beta}{-\frac{\Delta S_p - \Delta S_w}{R} + (D_p - D_w)T + \frac{\Delta E_p - \Delta E_w}{RT}} + 1 \right] \quad (8)$$

There are only small differences between numerical values of k_1 obtained from the above relation for HSA in solutions at pI in the whole range of temperatures: (0.775 ± 0.004) at 5°C and (0.782 ± 0.006) at 45°C . They are comparable with the values obtained earlier for BSA in solutions at pI (Monkos 1996): 0.711 ($t = 5^\circ\text{C}$) and 0.753 ($t = 45^\circ\text{C}$). However, they are lesser than those obtained for HSA at neutral pH (Monkos 2004). In this case the Huggins coefficient increases from 0.932 ($t = 5^\circ\text{C}$) up to 0.965 ($t = 45^\circ\text{C}$). The above presented results suggest that for a given protein k_1 reaches a minimum value in solutions at pI.

In many physical problems it is convenient to use dimensionless reduced variables. In the case of the viscosity-concentration dependence, such a reduced variable is a product of the intrinsic viscosity and concentration $[\eta]c$. The dependence of the specific viscosity on $[\eta]c$, presented in a log-log plot, shows for many macromolecules an existence of transition from dilute to semi-dilute solution at concentration c^* , and from semi-dilute to concentrated solution at a concentration c^{**} (Monkos 2000 and references therein). This is also the case for HSA in solutions at neutral pH (Monkos 2004). Such master curve for HSA in solutions at pI is, in turn, shown in Fig. 4. It has the same form over the whole range of measured temperatures. The parameters describing the curves are presented in Table 1.

In the dilute region ($[\eta]c < [\eta]c^*$) the plot of $\log \eta_{sp} - \log [\eta]c^*$ is linear. As is seen in Table 1 the boundary concentration c^* slightly increase with increasing temperature and the product $[\eta]c^*$ is – within the experimental errors – the same over the whole range of temperatures. It is worth to calculate the average distance $\langle r \rangle$ between the centers of two neighbouring proteins in this region. It is easy to show that $\langle r \rangle = (M_h/N_A)^{1/3}$. For the boundary concentration $c^* = (32.3 \pm 2.4) \text{ kg/m}^3$ ($t = 5^\circ\text{C}$): $\langle r \rangle = (16.8 \pm 0.4) \text{ nm}$ and for $c^* = (33.5 \pm 2.6) \text{ kg/m}^3$ ($t = 45^\circ\text{C}$): $\langle r \rangle = (16.6 \pm 0.4) \text{ nm}$. As has been mentioned above, the length of the long semi-axis of hydrated HSA molecule $a_h = 8.2 \text{ nm}$. This indicates that, in the region of dilute solutions, the average distance between the centers of

two neighbouring HSA molecules is nearly equal to or higher than the dimension of their long axis ($2a_h$). For HSA in solutions at neutral pH, the boundary concentration c^* increases from 37 kg/m^3 ($t = 5^\circ\text{C}$) up to 38.1 kg/m^3 ($t = 45^\circ\text{C}$), and the product $[\eta]c^*$ slightly decreases from 0.181 ($t = 5^\circ\text{C}$) up to 0.176 ($t = 45^\circ\text{C}$) (Monkos 2004). It means that the dilute region is slightly broader for HSA in solutions at pI. The slope of the straight line in the dilute region slowly decreases with increasing temperature (Table 1). For HSA in solutions at neutral pH the slope decreases from 1.1 ($t = 5^\circ\text{C}$) up to 1.09 ($t = 45^\circ\text{C}$) (Monkos 2004). It means that – for a given temperature – the slope is nearly identical for HSA in solutions both at neutral pH and at pI. The experiments conducted for quite different types of macromolecules showed that the slopes in the dilute domain are included in the range of 1.1–1.4 (Monkos 2000 and references therein).

In the dilute region the proteins move freely without interactions as in the infinitely diluted solutions. In the semi-dilute region ($[\eta]c^* < [\eta]c < [\eta]c^{**}$) the average distance between the centers of two neighbouring proteins becomes smaller than the length of their long axis, and besides electrostatic interactions the steric interactions appear. They arise because of impossibility of occupying by two molecules (or parts of molecules) the same point in space at the same time. As the solution concentration increases, the average distance between the centers of two neighbouring proteins decreases and the steric interactions become more distinct. In the semi-dilute region, the dependence of $\log\eta_{sp} - \log[\eta]c$ is non-linear (Fig. 4). It was previously observed for citrus pectins (Axelos et al. 1989), randomly coiled globular proteins (Lefebvre 1982) and native globular proteins (Monkos 1994, 2000, 2001, 2004). In this range of concentrations, the viscosity-concentration dependence can be described by the following equation (Lefebvre 1982):

$$\ln \eta_r = 2a [\eta]c^* \left(\frac{c}{c^*} \right)^{1/2a} - (2a - 1) [\eta]c^* \quad (9)$$

in which “a” is the Mark-Houwink-Kuhn-Sakurada (MHKS) exponent. This quantity depends on conformation of macromolecule in solution. For stiff macromolecules it does not depend on temperature. The experimentally obtained values of MHKS exponent for different types of macromolecules are as follows: $a = 0$ for hard spherical particles, $a < 0.5$ for compact quasi spherical molecules like native globular proteins, $0.5 < a < 1$ for random coils and $1.8 < a < 2$ for hard long rods (Monkos 2000 and references therein). Fig. 5 shows a plot of the relative viscosity vs. concentration in a log-normal plot, for HSA in solutions at pI and at 20°C , in a discussed region of concentrations. The curve shows the fit to the experimental values obtained by using Eq. (9), in which c^* and “a” were treated as adjustable parameters. On the other hand, the boundary concentration c^* can be immediately estimated from the master curve (Fig. 4). In both cases the values of c^*

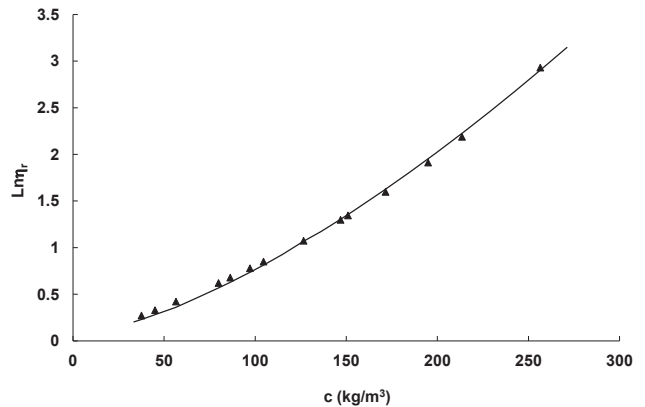


Figure 5. Plot of the relative viscosity versus concentration in a log-normal plot in a semi-dilute region for aqueous solutions of HSA at pH 4.7 and at temperature 20°C . The points were obtained from experimental values; the curve shows the fit obtained by using Eq. (9).

– obtained at the same temperature – are very similar. The parameters “a” and c^* , established by the above described method, are presented in Table 1. The MHKS exponent (Table 1), within the range of experimental errors, is nearly identical in the whole range of measured temperatures. This quantity obtained previously for HSA in solutions at neutral pH slightly decreases from 0.33 ($t = 5^\circ\text{C}$) up to 0.328 ($t = 45^\circ\text{C}$). However, within the experimental errors, the numerical values of MHKS exponent are in both cases nearly identical. It proves that HSA has the same conformation in solutions at neutral pH and at pI. The second boundary concentration c^{**} is, within the experimental errors, independent of temperature. This is also the case for the product $[\eta]c^{**}$. It means that for HSA in solutions at pI wideness of the semi-dilute region does not depend on temperature.

In the concentrated region ($[\eta]c > [\eta]c^{**}$), the plot of $\log\eta_{sp} - \log[\eta]c$ is again linear (Fig. 4). The average distance between the centers of two neighbouring proteins calculated in this region, in the whole range of temperatures, is nearly the same and is equal to $\langle r \rangle = 8.2 \text{ nm}$. It means, that in the concentrated region $\langle r \rangle$ is equal to (for $c = c^{**}$) or less than (for $c > c^{**}$) the length of the long semi-axis of the hydrated HSA molecule a_h . Nearly identical conclusion has been formulated for HSA in solutions at neutral pH (Monkos 2004). In the concentrated region the molecules of HSA are very close to each other and the movements of the molecules become partially correlative. The intermolecular interactions are dominated by the so called entanglement effects. As has been experimentally proved by some authors (Monkos 2000 and references therein), the slope in the $\log\eta_{sp} - \log[\eta]c$ plot in this region is a measure of macromolecular stiffness in a solution. For HSA in solutions at neutral pH the slope in this region decreases from 8.01 (5°C) up to 7.08 (45°C)

(Monkos 2004), and is (within the experimental errors) nearly the same as for HSA in solutions at pI (Table 1). For stiff molecules, the slope in the concentrated region should be equal to 8 (Baird and Ballman 1979). The obtained results show, that HSA molecules in solutions, both at neutral pH and at pI, are not perfectly stiff; their stiffness decreases with increasing temperature. However, it is worth to emphasize that this relative stiffness of HSA is necessary to performances its physiological functions in the circulatory system.

Conclusions

The viscosity-temperature dependence of HSA solutions at temperatures ranging from 5°C to 45°C – both at neutral pH and at isoelectric point – may be quantitatively described by a modified Arrhenius equation (Eq. 1). The parameters in this equation, i.e. the activation energy of viscous flow, the entropy and parameter D_s for HSA solutions monotonically increase with increasing concentration. Functional dependence of these parameters on concentration allow the calculation of the activation energy, entropy, parameter D_p and the effective specific volume for hydrated HSA. Analysis of these quantities shows that for HSA the activation energy, entropy, parameter D_p reach a maximum and the effective specific volume a minimum value at pI. The self-crowding factor is proportional to the effective specific volume of the protein and reaches also a minimum value in solutions at pI. For small concentrations, proteins solutions can be characterized by the intrinsic viscosity and Huggins coefficient. It appears that, for a given temperature, the intrinsic viscosity reaches a maximum and the Huggins coefficient a minimum value for HSA at pI. The plot of $\log\eta_{sp} - \log[\eta]c$ shows that for HSA – both at neutral pH and at pI – the three ranges of concentrations exist: diluted, semi-diluted and concentrated. The MHKS exponent, calculated from Lefebvre's equation in the semi-dilute region is, within the experimental errors, nearly the same for HSA both at neutral pH and at pI. The slope of the $\log\eta_{sp} - \log[\eta]c$ plot in the concentrated domain decreases with increasing temperature. It indicates that the stiffness of HSA molecules decreases with increasing temperature. Numerical values of the slope in this range, for a given temperature, are within the experimental errors the same in both cases. It proves that the conformation and stiffness of HSA molecules in solutions at neutral pH and at pI are the same.

Acknowledgments. This work was supported by the project of MUS: KNW-1-079/P/1/0.

References

- Abade G. C., Cichocki B., Ekiel-Jeżewska M. L., Nägele G., Wajnryb E. (2010a): Dynamics of permeable particles in concentrated suspensions. *Phys. Rev. E Stat. Nonlin. Soft. Matter. Phys.* **81**, 020404 <http://dx.doi.org/10.1103/PhysRevE.81.020404>
- Abade G. C., Cichocki B., Ekiel-Jeżewska M. L., Nägele G., Wajnryb E. (2010b): Short-time dynamics of permeable particles in concentrated suspensions. *J. Chem. Phys.* **132**, 014503 <http://dx.doi.org/10.1063/1.3274663>
- Abade G. C., Cichocki B., Ekiel-Jeżewska M. L., Nägele G., Wajnryb E. (2010c): High-frequency viscosity and generalized Stokes-Einstein relations in dense suspensions of porous particles. *J. Phys. Condens. Matter* **22**, 322101 <http://dx.doi.org/10.1088/0953-8984/22/32/322101>
- Abade G. C., Cichocki B., Ekiel-Jeżewska M. L., Nägele G., Wajnryb E. (2010d): High-frequency viscosity of concentrated porous particles suspensions. *J. Chem. Phys.* **133**, 084906 <http://dx.doi.org/10.1063/1.3474804>
- Abade G. C., Cichocki B., Ekiel-Jeżewska M. L., Nägele G., Wajnryb E. (2011): Rotational and translational self-diffusion in concentrated suspensions of permeable particles. *J. Chem. Phys.* **134**, 244903 <http://dx.doi.org/10.1063/1.3604813>
- Abade G. C., Cichocki B., Ekiel-Jeżewska M. L., Nägele G., Wajnryb E. (2012): Diffusion, Sedimentation, and rheology of concentrated suspensions of core-shell particles. *J. Chem. Phys.* **136**, 104902 <http://dx.doi.org/10.1063/1.3274663>
- Amiri M., Jankeje K., Albani J. R. (2010): Characterization of human serum albumin forms with pH. Fluorescence lifetime studies. *J. Pharm. Biomed. Anal.* **51**, 1097–1102 <http://dx.doi.org/10.1016/j.jpba.2009.11.011>
- Amoresano A., Andolfo A., Siciliano R. A., Cozzolino R., Minchietti L., Galliano M., Pucci P. (1998): Analysis of human serum albumin variants by mass spectrometric procedures. *Biochim. Biophys. Acta* **1384**, 79–92 [http://dx.doi.org/10.1016/S0167-4838\(97\)00223-9](http://dx.doi.org/10.1016/S0167-4838(97)00223-9)
- Ando T., Skolnick J. (2010): Crowding and hydrodynamic interactions likely dominate in vivo macromolecular motion. *Proc. Natl. Acad. Sci. U.S.A.* **107**, 18457–18462 <http://dx.doi.org/10.1073/pnas.1011354107>
- Antosiewicz J. (1995): Computation of the dipole moment of proteins. *Biophys. J.* **69**, 1344–1354 [http://dx.doi.org/10.1016/S0006-3495\(95\)80001-9](http://dx.doi.org/10.1016/S0006-3495(95)80001-9)
- Avramov I. (1998): Viscosity of glassforming melts. *J. Non-Cryst. Solids* **238**, 6–10 [http://dx.doi.org/10.1016/S0022-3093\(98\)00672-3](http://dx.doi.org/10.1016/S0022-3093(98)00672-3)
- Axelos M. A. V., Thibault J. F., Lefebvre J. (1989): Structure of citrus pectins and viscometric study of their solution properties. *Int. J. Biol. Macromol.* **11**, 186–191 [http://dx.doi.org/10.1016/0141-8130\(89\)90066-4](http://dx.doi.org/10.1016/0141-8130(89)90066-4)
- Baird D. G., Ballman R. L. (1979): Comparison of the rheological properties of concentrated solutions of a rodlike and a flexible chain polyamide. *J. Rheol.* **23**, 505–524 <http://dx.doi.org/10.1122/1.549530>
- Baranowska H. M., Olszewski K. J. (1996): The hydration of proteins in solutions by self-diffusion coefficients NMR study. *Biochim. Biophys. Acta* **1289**, 312–314 [http://dx.doi.org/10.1016/0304-4165\(95\)00141-7](http://dx.doi.org/10.1016/0304-4165(95)00141-7)
- Bhattacharya A. A., Grüne T., Curry S. (2000): Crystallographic analysis reveals common modes of binding of medium and long-chain fatty acids to human serum albumin. *J. Mol. Biol.* **303**, 721–732

- <http://dx.doi.org/10.1006/jmbi.2000.4158>
- Bramanti E., Benedetti E. (1994): Determination of the secondary structure of isomeric forms of human serum albumin by a particular frequency deconvolution procedure applied to Fourier transform IR analysis. *Biopolymers* **38**, 639–653
[http://dx.doi.org/10.1002/\(SICI\)1097-0282\(199605\)38:5<639::AID-BIP8>3.0.CO;2-T](http://dx.doi.org/10.1002/(SICI)1097-0282(199605)38:5<639::AID-BIP8>3.0.CO;2-T)
- Buzády A., Erostyák J., Somogyi B. (2001): Phase-fluorometry study on dielectric relaxation of acrylodan-labeled human serum albumin. *Biophys. Chem.* **94**, 75–85
[http://dx.doi.org/10.1016/S0301-4622\(01\)00212-5](http://dx.doi.org/10.1016/S0301-4622(01)00212-5)
- Chilom C. G., Barangă G., Găzdaru D. M., Popescu A. (2011): A spectroscopic approach of pH effect on thermal denaturation of human and bovine serum albumins. *J. Optoelet. Adv. Materials* **13**, 583–587
- Dockal M., Carter D. C., Rüker F. (1999): The three recombinant domains of human serum albumin. *J. Biol. Chem.* **274**, 29303–29310
<http://dx.doi.org/10.1074/jbc.274.41.29303>
- Ferrer M. L., Duchowich R., Carrasco, B., Garcia de la Torre J., Acuña A.U. (2001): The conformation of serum albumin in solution: a combined phosphorescence depolarization-hydrodynamic modeling study. *Biophys. J.* **80**, 2422–2430
[http://dx.doi.org/10.1016/S0006-3495\(01\)76211-X](http://dx.doi.org/10.1016/S0006-3495(01)76211-X)
- Gapinski J., Patkowski A., Banchio A. J., Holmqvist P., Meier G., Lettinga M. P., Nägele G. (2007): Collective diffusion in charge-stabilized suspensions: concentration and salt effects. *J. Chem. Phys.* **126**, 104905
- Gelamo E. L., Silva C. H. T. P., Imasato H., Tabak M. (2002): Interaction of bovine (BSA) and human (HSA) serum albumins with ionic surfactants: spectroscopy and modeling. *Biochim. Biophys. Acta* **1594**, 84–99
[http://dx.doi.org/10.1016/S0167-4838\(01\)00287-4](http://dx.doi.org/10.1016/S0167-4838(01)00287-4)
- He X. M., Carter D. C. (1992): Atomic structure and chemistry of human serum albumin. *Nature* **358**, 209–215
<http://dx.doi.org/10.1038/358209a0>
- Heinen M., Zanini F., Rooses-Runge F., Fedunová D., Zhang F., Henning M., Seydel T., Schweins R., Sztucki M., Analík M., Schreiber F., Nägele G. (2012): Viscosity and diffusion: crowding and salt effects in protein solutions. *Soft Matter* **8**, 1404–1419
<http://dx.doi.org/10.1039/c1sm06242e>
- Holmqvist P., Nägele G. (2010): Long-time dynamics of concentrated charge-stabilized colloids. *Phys. Rev. Lett.* **104**, 058301
- Junk M. J. N., Spiess H. W., Hinderberger D. (2011): Characterization of the solution structure of human serum albumin loaded with a metal porphyrin and fatty acids. *Biophys. J.* **100**, 2293–2301
<http://dx.doi.org/10.1016/j.bpj.2011.03.050>
- Kamal J. K. A., Behere D. V. (2002): Spectroscopic studies on human serum albumin and methemalbumin: optical, steady-state, and picosecond time-resolved fluorescence studies, and kinetics of substrate oxidation by methemalbumin. *J. Biol. Inorg. Chem.* **7**, 273–283
<http://dx.doi.org/10.1007/s007750100294>
- Laberge M. (1998): Intrinsic protein electric fields: basic non-covalent interactions and relationship to protein-induced Stark effects. *Biochim. Biophys. Acta* **1386**, 305–330
[http://dx.doi.org/10.1016/S0167-4838\(98\)00100-9](http://dx.doi.org/10.1016/S0167-4838(98)00100-9)
- Ladam G., Gergely C., Senger B., Decher G., Voegel J-C., Schaaf P., Cuisinier F. J. G. (2000): Proton interactions with polyelectrolyte multilayers: interactions between human serum albumin and polystyrene sulfonate/polyallylamine multilayers. *Biomacromolecules* **1**, 674–687
<http://dx.doi.org/10.1021/bm005572q>
- Lefebvre J. (1982): Viscosity of concentrated protein solutions. *Rheol. Acta* **21**, 620–625
<http://dx.doi.org/10.1007/BF01534361>
- Matei I., Ionescu S., Hillebrand M. (2011): Interaction of fisetin with human serum albumin by fluorescence, circular dichroism spectroscopy and DFT calculations: binding parameters and conformational changes. *J. Lumin.* **131**, 1629–1635
<http://dx.doi.org/10.1016/j.jlumin>
- Menon R. S., Allen P. S. (1990): Solvent proton relaxation of aqueous solutions of the serum proteins α 2 – macroglobulin, fibrinogen, and albumin. *Biophys. J.* **57**, 389–396
[http://dx.doi.org/10.1016/S0006-3495\(90\)82555-8](http://dx.doi.org/10.1016/S0006-3495(90)82555-8)
- Monkos K. (1994): Viscometric study of human, bovine, equine and ovine haemoglobin in aqueous solution. *Int. J. Biol. Macromol.* **16**, 31–35
[http://dx.doi.org/10.1016/0141-8130\(94\)90008-6](http://dx.doi.org/10.1016/0141-8130(94)90008-6)
- Monkos K. (1996): Viscosity of bovine serum albumin aqueous solutions as a function of temperature and concentration. *Int. J. Biol. Macromol.* **18**, 61–68
[http://dx.doi.org/10.1016/0141-8130\(95\)01057-2](http://dx.doi.org/10.1016/0141-8130(95)01057-2)
- Monkos K. (1997): Concentration and temperature dependence of viscosity in lysozyme aqueous solutions. *Biochim. Biophys. Acta* **1339**, 304–310
[http://dx.doi.org/10.1016/S0167-4838\(97\)00013-7](http://dx.doi.org/10.1016/S0167-4838(97)00013-7)
- Monkos K. (2000): Viscosity analysis of the temperature dependence of the solution conformation of ovalbumin. *Biophys. Chem.* **85**, 7–16
[http://dx.doi.org/10.1016/S0301-4622\(00\)00127-7](http://dx.doi.org/10.1016/S0301-4622(00)00127-7)
- Monkos K. (2001): Temperature dependence of the Mark-Houwink-Kuhn-Sakurada exponent for lysozyme in aqueous solutions. *Curr. Top. Biophys.* **25**, 75–80
- Monkos K. (2004): On the hydrodynamics and temperature dependence of the solution conformation of human serum albumin from viscometry approach. *Biochim. Biophys. Acta* **1700**, 27–34
<http://dx.doi.org/10.1016/j.bbapap.2004.03.006>
- Monkos K. (2005a): A comparison of solution conformation and hydrodynamic properties of equine, porcine and rabbit serum albumin using viscometric measurements. *Biochim. Biophys. Acta* **1748**, 100–109
<http://dx.doi.org/10.1016/j.bbapap.2004.12.008>
- Monkos K. (2005b): Determination of some hydrodynamic parameters of ovine serum albumin solutions using viscometric measurements. *J. Biol. Phys.* **31**, 219–232
<http://dx.doi.org/10.1007/s10867-005-1830-z>
- Monkos K. (2011): Temperature behaviour of viscosity flow with proteins. *Gen. Physiol. Biophys.* **30**, 121–129
http://dx.doi.org/10.4149/gpb_2011_02_121
- Monkos K., Turczynski B. (1991): Determination of the axial ratio of globular proteins in aqueous solution using viscometric measurements. *Int. J. Biol. Macromol.* **13**, 341–344

- [http://dx.doi.org/10.1016/0141-8130\(91\)90015-M](http://dx.doi.org/10.1016/0141-8130(91)90015-M)
- Monkos K., Turczynski B. (1999): A comparative study on viscosity of human, bovine and pig IgG immunoglobulins in aqueous solutions. *Int. J. Biol. Macromol.* **26**, 155–159
[http://dx.doi.org/10.1016/S0141-8130\(99\)00080-X](http://dx.doi.org/10.1016/S0141-8130(99)00080-X)
- Mooney M. J. (1951): The viscosity of a concentrated suspension of spherical particles. *J. Colloid Sci.* **6**, 162–170
[http://dx.doi.org/10.1016/0095-8522\(51\)90036-0](http://dx.doi.org/10.1016/0095-8522(51)90036-0)
- Moser P., Squire P. G., O'Konski C. T. (1966): Electric polarization in proteins – dielectric dispersion and Kerr effect. Studies of isoionic bovine serum albumin. *J. Phys. Chem.* **70**, 744–756
<http://dx.doi.org/10.1021/j100875a023>
- Olivieri J. R., Craievich A. F. (1995): The subdomain structure of human serum albumin in solution under different pH conditions studied by small angle X-ray scattering. *Eur. Biophys. J.* **24**, 77–84
- Otosu T., Nishimoto E., Yamashita S. (2010): Multiple conformational state of human serum albumin around single tryptophan residue at various pH revealed by time-resolved fluorescence spectroscopy. *J. Biochem.* **147**, 191–200
<http://dx.doi.org/10.1093/jb/mvp175>
- Pamies R., Cifre J. G. H., Martinez M. C. L., Garcia de la Torre J. (2008): Determination of intrinsic viscosities of macromolecules and nanoparticles. Comparison of single-point and dilution procedures. *Colloid. Polym. Sci.* **286**, 1223–1231
<http://dx.doi.org/10.1007/s00396-008-1902-2>
- Peters T. (1985): Advances in Protein Chemistry. Vol. 37, pp.161–245, Academic Press, New York
[http://dx.doi.org/10.1016/S0065-3233\(08\)60065-0](http://dx.doi.org/10.1016/S0065-3233(08)60065-0)
- Peters T. Jr. (1996): Metabolism: Albumin in the body. In: All about Albumin. Biochemistry, Genetics, and Medical Applications. (Ed. T. Peters), pp. 188–250, Academic Press Limited
- Picó G. A. (1997): Thermodynamic features of the thermal unfolding of human serum albumin. *Int. J. Biol. Macromol.* **20**, 63–73
[http://dx.doi.org/10.1016/S0141-8130\(96\)01153-1](http://dx.doi.org/10.1016/S0141-8130(96)01153-1)
- Pouliquen D., Gallois Y. (2001): Physicochemical properties of structures water in human albumin and gammaglobulin solutions. *Biochimie* **83**, 891–898
[http://dx.doi.org/10.1016/S0300-9084\(01\)01330-X](http://dx.doi.org/10.1016/S0300-9084(01)01330-X)
- Reiss H. (1965): Scaled particle methods in the statistical thermodynamics of fluids. *Advan. Chem. Phys.* **9**, 1–84
<http://dx.doi.org/10.1002/9780470143551.ch1>
- Roosen-Runge F., Hennig M., Zhang F., Jacobs R. M. J., Sztucki M., Schober H., Seydel T., Schreiber F. (2011): Protein self-diffusion in crowded solutions. *Proc. Natl. Acad. Sci. USA* **108**, 11815–11820
<http://dx.doi.org/10.1073/pnas.1107287108>
- Sjöberg B., Mortensen K. (1994): Interparticle interactions and structure in nonideal solutions of human serum albumin studied by small-angle neutron scattering and Monte Carlo simulation. *Biophys. Chem.* **52**, 131–138
[http://dx.doi.org/10.1016/0301-4622\(94\)00089-1](http://dx.doi.org/10.1016/0301-4622(94)00089-1)
- Sontum P. C., Christiansen C. (1997): Photon correlation spectroscopy applied to characterization of denaturation and thermal stability of human albumin. *J. Pharm. Biomed. Anal.* **16**, 295–302
[http://dx.doi.org/10.1016/S0731-7085\(97\)00032-0](http://dx.doi.org/10.1016/S0731-7085(97)00032-0)
- Squire P. G., Himmel M. E. (1979): Hydrodynamics and protein hydration. *Arch. Biochem. Biophys.* **196**, 165–177
[http://dx.doi.org/10.1016/0003-9861\(79\)90563-0](http://dx.doi.org/10.1016/0003-9861(79)90563-0)
- Svergun D. I., Richard S., Koch M. H. J., Sayers Z., Kuprin S., Zaccai G. (1998): Protein hydration in solution: Experimental observation by x-ray and neutron scattering. *Proc. Natl. Acad. Sci. U.S.A.* **95**, 2267–2272
<http://dx.doi.org/10.1073/pnas.95.5.2267>
- Tukuyama M., Oppenheim I. (1995a): On the theory of concentrated hard-sphere suspensions. *Physica A* **216**, 85–119
[http://dx.doi.org/10.1016/0378-4371\(94\)00280-7](http://dx.doi.org/10.1016/0378-4371(94)00280-7)
- Tukuyama M., Oppenheim I. (1995b): Dynamics of self-diffusion process in concentrated hard-sphere suspensions of interacting Brownian particles. *J. Korean Phys. Soc.* **28**, S327–332
- Vilker V. L., Colton C. K., Smith K. A. (1981): The osmotic pressure of concentrated protein solutions: effect of concentration and pH in saline solutions of bovine serum albumin. *J. Colloid. Interface Sci.* **79**, 548–566
[http://dx.doi.org/10.1016/0021-9797\(81\)90106-5](http://dx.doi.org/10.1016/0021-9797(81)90106-5)
- Vinogradov G. V., Malkin A. Ya. (1980): Rheology of Polymers. Mir Publishers, Moscow
- Vlasova I. M., Bukharova E. M., Kuleshova A. A., Saletsky A. M. (2011): Spectroscopic investigations of interaction of fluorescent nanomarkers of fluorescein family with human serum albumin at different values of pH. *Cur. Appl. Phys.* **11**, 1126–1132
<http://dx.doi.org/10.1016/j.cap.2011.02.004>
- Vlasova I. M., Saletsky A. M. (2009): Investigation of influence of different values of pH on mechanisms of binding of human serum albumin with markers of fluorescein family. *J. Mol. Struct.* **936**, 220–227
<http://dx.doi.org/10.1016/j.molstruc.2009.07.043>
- Vlasova I. M., Vlasov A. V., Saletsky A. M. (2010): Interaction of ionic detergent cetyltrimethyl ammonium bromide with human serum albumin at various values of pH: Spectroscopic study. *J. Mol. Struct.* **984**, 332–338
<http://dx.doi.org/10.1016/j.molstruc.2010.09.051>
- Vos K., van Hoek A., Visser A. J. W. G. (1987): Application of a reference convolution method to tryptophan fluorescence in proteins. *Eur. J. Biochem.* **165**, 55–63
<http://dx.doi.org/10.1111/j.1432-1033.1987.tb11193.x>
- Young E. G. (1963): Occurrence, classification, preparation and analysis of proteins. In: Comprehensive Biochemistry (Eds. M. Florkin and E.H. Stoltz), Vol. 7, pp. 1–53, Elsevier, Amsterdam
- Zimmerman S. B., Minton A. P. (1993): Macromolecular crowding: biochemical, biophysical, and physiological consequences. *Annu. Rev. Biophys. Biomol. Struct.* **22**, 27–65
<http://dx.doi.org/10.1146/annurev.bb.22.060193.000331>
- Zimmerman S. B., Trach S. O. (1991): Estimation of macromolecule concentrations and excluded volume effects for the cytoplasm of Escherichia coli. *J. Mol. Biol.* **222**, 599–620
[http://dx.doi.org/10.1016/0022-2836\(91\)90499-V](http://dx.doi.org/10.1016/0022-2836(91)90499-V)

Received: February 28, 2012

Final version accepted: June 6, 2012